ABOVEGROUND THERMODYNAMIC OBSERVATIONS IN CONVECTIVE STORMS FROM BALLOONBORNE PROBES ACTING AS PSEUDO-LAGRANGIAN DRIFTERS

Paul M. Markowski, Yvette P. Richardson, Scott J. Richardson, and Anders Petersson

Critical, hard-to-get observations in severe thunderstorms are obtained via a novel use of balloonborne probes.

A great deal already is known about the dynamics and prediction of severe convective storms from observational, theoretical, and numerical simulation studies. Environments capable of supporting tornado outbreaks or derechos frequently are predicted by the Storm Prediction Center days in advance, strong tornadoes (EF2 or higher on the enhanced Fujita scale) rarely occur outside of tornado watches, and forecasts of the development of dangerous storms sometimes even trigger early dismissals from schools. The latter is testament of the tremendous public confidence in today's convective storm forecasts. Predictions are bound to get even better, especially in the 0–1-h time frame, owing to the continually improving ability to run simulations on increasingly fine, convection-resolving grids. Having said this, there will always be room for improvements in our physical understanding of storms. For example, it is vital to know "how storms work" if one is to improve the parameterizations in storm simulations or evaluate the credibility of a numerical prediction. Observations will forever be important in this venture. This paper is about a notable gap in our ability to observe the thermodynamic characteristics of convective storms and describes a new way to obtain these important observations.

Radars are arguably the most important tool in severe storms research and operations. Nothing beats radar when it comes to assessing the structure of storms. From reflectivity observations alone, one can typically infer the locations of the heaviest precipitation; the most likely locations of large hail, updrafts, and downdrafts; and even the presence of rotation.

AFFILIATIONS: Markowski, Richardson, and Richardson—Department of Meteorology and Atmospheric Science, The Pennsylvania State University, University Park, Pennsylvania; Petersson—Sparv Embedded AB, Linköping, Sweden
CORRESPONDING AUTHOR: Paul M. Markowski, pmarkowski@psu.edu

The abstract for this article can be found in this issue, following the table of contents.
DOI:10.1175/BAMS-D-17-0204.1

In final form 9 October 2017

Radial velocity observations afforded by a Doppler radar provide additional information, such as the magnitude of the wind shear associated with azimuthal and radial variations of inbound and outbound radial velocities. If Doppler radar observations are collected approximately contemporaneously from two or more radars (so-called dual-Doppler observations), assuming the radar beams intersect at sufficiently large angles, the three-dimensional wind fields can be retrieved. Three-dimensional wind fields allow one to assess valuable parameters such as vorticity and convergence, and a time series of three-dimensional winds permits trajectories to be computed.

However, in order to understand *why* a storm evolves as observed (which could include how a tornado forms or how a squall line is maintained), one must know the *forces* responsible for wind accelerations, such as pressure-gradient and buoyancy forces. Determining the forces requires thermodynamic observations, that is, information about the temperature, moisture, and pressure fields. These observations are not directly available from radars. Although dozens of dual-Doppler datasets have been obtained by mobile radars in convective storms in field projects (e.g., Wakimoto and Atkins 1996; Wakimoto et al. 1998; Trapp 1999; Wakimoto and Cai 2000; Ziegler et al. 2001; Dowell and Bluestein 2002; Beck et al. 2006; Wurman et al. 2007a,b, 2010; Marquis et al. 2008, 2012; Frame et al. 2009; Markowski et al. 2011, 2012; Kosiba et al. 2013; Calhoun et al. 2013; Potvin et al. 2013; Skinner et al. 2014; Davenport and Parker 2015; Klees et al. 2016; Betten et al. 2017), complementary thermodynamic observations mostly have been limited to in situ measurements by automobiles, termed mobile mesonets (Straka et al. 1996; Waugh and Fredrickson 2010), and rapidly deployable surface stations, such as the Texas Tech University StickNet (Weiss and Schroeder 2008). Although pressure and buoyancy fields can be retrieved from dual-Doppler-derived wind fields (e.g., Gal-Chen 1978; Hane et al. 1981; Brandes 1984; Hauser et al. 1988), the retrieved fields (especially buoyancy) have not been found to be sufficiently accurate for the quantitative study of severe convective storms, owing to the large sensitivity of the retrievals to observation errors and boundary conditions (e.g., Majcen et al. 2008). Buoyancy retrievals are especially error prone owing to their sensitivity to vertical gradients of retrieved pressure and the time derivative of the vertical velocity field. The latter is poorly assessed given that a few minutes typically elapse between the volumes of retrieved wind fields, and retrieved vertical velocity is itself error prone. Moreover, rapid evolution of the wind fields (especially if a tornado is developing) is common, which is problematic for not just the retrievals of pressure and buoyancy, but also the retrieval of the wind field.

Of greatest interest are thermodynamic observations within the cold pools of storms, where horizontal buoyancy gradients are potentially large and substantial amounts of vorticity can be generated [the lowest 2500 m above ground level (AGL) are probably of greatest interest]. The depth and magnitude of the negative buoyancy (and implied horizontal vorticity generation) within the cold pools of mesoscale convective systems (MCSs) strongly influence MCS structure, maintenance, and the likelihood of damaging winds (e.g., Rotunno et al. 1988; Coniglio and Stensrud 2001; Weisman and Rotunno 2004, 2005; Stensrud et al. 2005; James et al. 2006; Engerer et al. 2008; Bryan and Parker 2010). The vertically integrated buoyancy within the cold pool matters much more than the buoyancy next to the surface (Rotunno et al. 1988). In supercell thunderstorms, tornado formation is sensitive to the negative buoyancy and equivalent potential temperature of the rain-cooled, vorticity-rich air that emanates from downdrafts (e.g., Markowski and Richardson 2009, 2014; Davies-Jones 2015), with tornadogenesis likelihood generally increasing as buoyancy and equivalent potential temperature increase within the rain-cooled, vorticity-rich air—*at least near the surface* (e.g., Markowski et al. 2002; Grzych et al. 2007; Hirth et al. 2008; Snook and Xue 2008; Markowski and Richardson 2014). Reliable thermodynamic observations *above the ground* have been conspicuously missing. Knowledge of the thermodynamic fields above the ground is valuable, for example, because the air feeding the tornado (or developing tornado) descends to the surface in downdrafts prior to entering the circulation; thus, it is above the ground just minutes earlier. The horizontal buoyancy gradients influence the rate of horizontal vorticity generation, and this vorticity can become vertical through vorticity tilting.

Thermodynamic observations above the ground within the cold pools of storms have been elusive. Remote sensing platforms (e.g., Raman lidars, radiometers), either ground based, airborne, or spaceborne, are not particularly useful owing to the relatively long times required to complete a scan and the inability to penetrate clouds and precipitation. Surface-based observing systems have enabled great strides in our understanding of the importance of the thermodynamic characteristics in tornadogenesis (e.g., Markowski et al. 2002; Shabbott and Markowski 2006; Grzych et al. 2007; Hirth et al. 2008; Markowski et al. 2012; Weiss et al. 2015), though such ground-based observations can only provide information at

the bottom of the trajectories that enter a developing and/or mature tornado—trajectories that spend a considerable time aloft prior to reaching the surface—and only where there are roads.

In recent years, airborne observations have been obtained in supercell storms from unmanned aeronautical vehicles (UAVs; e.g., Houston et al. 2012; Riganti and Houston 2017), but such observations are extremely difficult to obtain in the most hazardous parts of storms, which also tend to be the most scientifically interesting. These include the area immediately north and northeast of a supercell storms mesocyclone, which is characterized by heavy rain, large hail, severe turbulence, and low visibility. In addition to the hostile flying conditions, the Federal Aviation Administration (FAA) requires that visual contact be maintained with the UAV at all times.

Dropsondes are another likely candidate, and they have been used successfully to sample the cold pools of MCSs (e.g., Correia and Arritt 2008). However, they are expensive, particularly when considering the cost of the flight time for the mother aircraft, and their use over land is highly restricted by the FAA. Latitudes and longitudes need to be identified well in advance, and drops are permitted only in relatively remote areas and at certain times of day. For the study of supercells, which are much smaller than MCSs, it would be difficult to get dropsondes into key areas (e.g., within the supercell's forward-flank and rear-flank downdrafts) even without FAA restrictions. If flying at low altitudes, the mother aircraft might be unable to fly through the accompanying harsh environments (e.g., heavy rain, large hail, and severe turbulence). The aircraft could instead drop probes from a less hostile atmosphere at high altitudes above the storm (above ~15 km AGL). However, the faster airspeed required of the aircraft and large vertical shear within and near the storm (the horizontal velocity differential over the depth of a dropsonde's flight could exceed 50 m s^{-1}) might make it difficult for dropsondes to "hit their marks."

Using numerical simulations to explore the range of thermodynamic characteristics within storms is problematic as well, owing to the great sensitivity of the temperature and precipitation fields to the microphysics parameterization (e.g., Gilmore et al. 2004; Snook and Xue 2008; Dawson et al. 2010, 2015; Bryan and Morrison 2012). It is not a stretch to say that an investigator can obtain almost any low-level buoyancy field in a simulated thunderstorm that she or he wants, simply by tuning the models microphysics parameterization.

Observations of the three-dimensional thermodynamic fields might also prove to be crucial for assessing the contribution of frictionally generated horizontal vorticity to the development of vortices in convective storms. This has been a hot topic in the severe storms community lately (Schenkman et al. 2012, 2014; Xu et al. 2015; Roberts et al. 2016) and unfortunately one that is exceptionally difficult to study both observationally and with simulations. Observational studies of the effects of surface friction are problematic because one cannot know how an observed storm might have behaved differently if in a frictionless setting. Storm simulations with surface friction are problematic because the lower boundary conditions assume a logarithmic vertical wind profile next to the surface, an assumption that is likely unjustified in convective storms. However, it might be possible to assess the effects of surface friction (and viscous effects in general) on vorticity indirectly as a residual using credible three-dimensional wind and thermodynamic fields to compute the vorticity forcings not related to friction.

In summary, reliable, aboveground, thermodynamic observations in convective storms are desperately needed. These missing observations, and the errors/uncertainty in the thermodynamic fields of simulated storms, are routinely cited as being among the most important hurdles to further our understanding of vorticity generation in supercell storms, as well as addressing many key aspects of MCSs, such as their maintenance and production of damaging winds.

"TWO BALLOON" RAWINSONDES AS PSEUDO-LAGRANGIAN DRIFTERS. At The Pennsylvania State University (Penn State), we have partnered with Sparv Embedded, a small company based in Linköping, Sweden, in the pursuit of aboveground thermodynamic observations in storms via the deployment of two-balloon rawinsondes (commercially the probes go by the name Swarmsonds). Two small helium-filled balloons, each only approximately 24 in. in diameter (less than 1/20 the volume of a standard weather balloon), are attached to a small, lightweight (13 g) sonde. After ascending to some "separation altitude," which most often was set to 500–1500 m for our storm intercepts (the altitude can be set before launch or anytime during flight), one of the balloons is released, leaving behind an approximately neutrally buoyant sonde supported by the remaining balloon, resulting in a pseudo-Lagrangian drifter.[1] As of May 2017, we could track up to 34 drifters simultaneously using two receivers operating on two different frequencies.

[1] This use of Sparv Embedded's two-balloon sondes is the brainchild of author S. Richardson.

Each probe reports temperature, pressure, and relative humidity at 2-s intervals; GPS latitude and longitude at 6-s intervals; and GPS altitude at 12-s intervals. The rationale behind the position being transmitted less frequently than the state variables is the desire to use as little bandwidth as possible; it has been assumed that it is sufficient to update position less often than the state variables. Position errors resulting from linear interpolation every 6 (12) s for latitude and longitude (altitude) are unlikely to be more than a few meters, barring wild accelerations. Such errors are small relative to the along-trajectory and cross-trajectory temperature–humidity–pressure data spacings, respectively, of ~30–50 m (for 15–25 m s^{-1} horizontal winds and 2-s updates) and ~500–1000 m (cross-trajectory resolution is dictated by the number of sondes and the wind fields through which they drift). Though they were not used herein, speed and heading data are also transmitted at 2-s intervals, and could be used to improve position estimates between the latitude, longitude, and altitude updates. A higher-order interpolation could be used as well.

The temperature, pressure, and relative humidity errors are 0.3°C, 0.3–0.5 hPa, and 5%, respectively. The temperature and relative humidity sensors are protected by a small radiation and precipitation shield. When the probe has a vertical velocity relative to the air of 2–3 m s^{-1}, the response time for temperature and relative humidity is approximately 5 s. For slower air-relative velocities, the response time would be slower, but we cannot yet quantify this; we suspect the sondes might typically experience a ~1 m s^{-1} wind, even when the balloon is moving as a perfect Lagrangian drifter (more on this below), owing to the sonde swinging beneath the balloon. This is an area in which more research and testing are needed.

Communications between the sondes and receiver typically are maintained out to ranges of 50–75 km, depending on the line of sight, and for 45–60 min, which corresponds to the typical life of the 3.7-V, 75-mAh polymer lithium batteries that power the probes. Additional details about all aspects of the probes can be found on Sparv Embedded's websites (http://sparvembedded.com/, www.windsond.com). There are no known FAA restrictions, as is the case for traditional mobile soundings launched in any field project.

Extensive testing was conducted in the autumn of 2016 in Pennsylvania in order to determine the balloon sizes needed to obtain the desired vertical velocities with one and two balloons attached to the sonde, and to assess how precipitation might affect vertical velocities. Two helium-filled balloons of approximately 24-in. (60 cm) diameter yield an ascent rate that is typically 3–5 m s^{-1} in precipitation-free conditions (the range of vertical velocities is a reflection of the typical vertical velocity variations found in the atmospheric boundary layer), and following the release of one of the balloons, the vertical velocity tends to be in the 0–2 m s^{-1} range in precipitation-free air. Once in the storm (and once one balloon has been released), probe vertical velocities can range from several meters per second downward to slightly positive, depending on the strength of the storm-scale downdrafts and precipitation intensity (water that accumulates on the balloon, as well as the momentum transferred from falling raindrops to the balloon, contribute to negative vertical velocity). Thus, even though we have precise control over when to release one balloon, we have only limited control over the exact altitude at which the probes will fly through a storm. Getting the probes to sample the parts of the storm of greatest scientific interest is necessarily a bit of an art. The balloonborne probes are referred to as "pseudo Lagrangian" drifters given that the probes are not exactly neutrally buoyant.[2]

In addition to the aforementioned tests, numerical simulations were performed in which synthetic two-balloon probe trajectories through simulated supercell storms were used to inform our launching strategy (Fig. 1); that is, the optimal storm-relative position from which to launch probes and the optimal height at which to jettison the first balloon. Although the balloons are not steerable like UAVs, the storm's own internal wind field can be used to pull the balloon through the key parts of the storm in which observations are so desperately needed. For the environmental wind fields most likely to be observed near a supercell thunderstorm, the storm-relative winds at low levels tend to blow toward the storm from the east or southeast, and the simulations suggested launching the probes from a position 5–20 km upwind of the storm's so-called forward-flank precipitation region, which is typically east or southeast of the edge of the precipitation. Probes launched from this location tend to be readily drawn through the precipitation and downdraft region (i.e., the most scientifically interesting part of the storm, as explained in the first section by the storm's own internal wind field, sampling the critical three-dimensional thermodynamic fields along the way. Moreover, this can be accomplished while keeping crews outside the region of harsh weather conditions, greatly increasing the probability of success

[2] A perfect Lagrangian drifter would have limited aspiration (it would be limited to the swinging of the sonde beneath the balloon), which could be problematic.

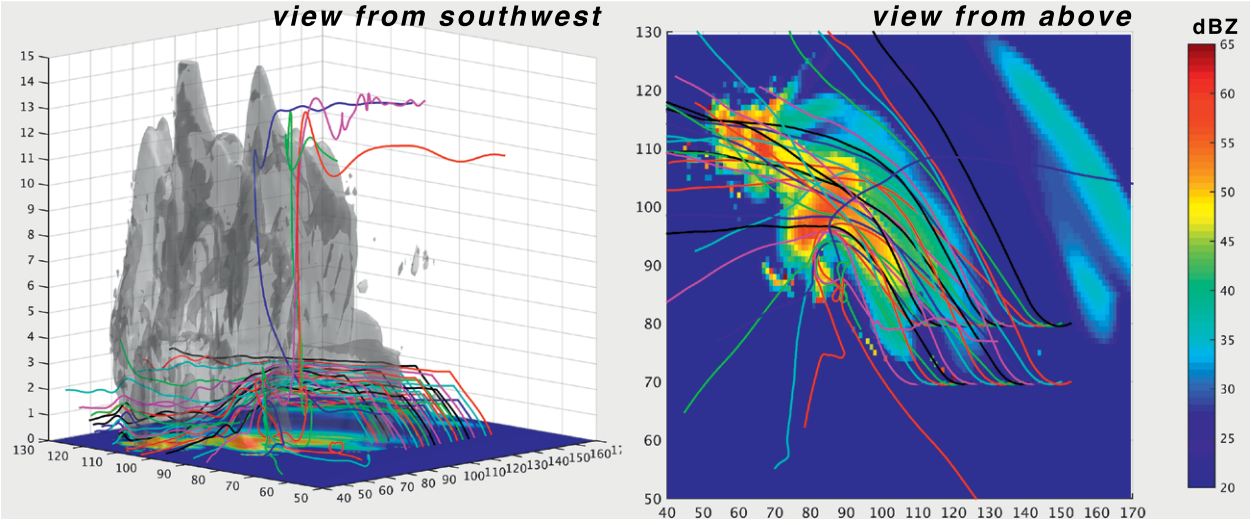

Fig. 1. Example of a simulation in which probes were tracked through an eastward-moving supercell thunderstorm (the probe trajectories are storm relative). Probes were "launched" in the simulation every 3 min for 90 min from two vans separated by 10 km along a hypothetical north–south road, using separation altitudes of 1.5, 2.0, and 2.5 km (a range of colors is used simply to allow individual trajectories to be more easily seen). Numbers along the axes are distances (km). (left) The gray isosurface is 30 dBZ. A horizontal cross section of radar reflectivity at an altitude of 500 m is displayed beneath the trajectories in both panels.

(note in Fig. 1 that not a single launch occurs in reflectivity exceeding 30 dB*Z*).[3]

The presence of storm-relative winds (which, equivalently, implies precipitation-relative and downdraft-relative winds) is key; significant storm-relative flow is what allows the probes to be drawn through the storm's areas of interest, as opposed to simply moving along at the same velocity as features of interest, never to actually pass through them. Significant storm-relative winds require the presence of significant wind shear in the environment. Fortunately, strong wind shear is one of the ingredients of severe thunderstorm environments. In other words, we can count on significant storm-relative flow to be present within the storms of greatest interest.

FIELD TESTING IN MAY 2017. Following the fall 2016 test period and numerical simulation studies, storm intercepts with the two-balloon sondes were attempted in the Great Plains region in late May 2017, which coincided with a small field project led by the National Severe Storms Laboratory (NSSL) coined Rivers of Vorticity in Supercells (RiVorS). Probes were flown through supercell storms on 27 May near Mannsville, Oklahoma, and on 31 May near Ransom, Kansas. Each of these storms exhibited persistent rotation at midlevels, but only occasional rotation at low levels. Neither produced a tornado. These deployments are summarized below.

All of the probes were launched from a single passenger van with a crew of just two individuals (authors P. Markowski and Y. Richardson). The time that elapsed between successive launches was nearly 5 min at the start of the first deployment, but this time was reduced to less than 3 min by the end of the first deployment as the two operators gained experience and efficiency. The time that elapsed between launches was largely driven by the amount of time required to inflate two balloons and attach the balloons to the sondes.[4] It also could take up to a minute for each sonde's GPS receiver to lock on to GPS satellites, but this was done in parallel with balloon inflation. Batteries were fully charged and inserted into the sondes days prior to the deployment. In the future,

[3] To collect in situ, airborne observations near a tornado for the 1996 film *Twister*, the characters portrayed by actors Bill Paxton and Helen Hunt resorted to placing their pickup truck in cruise control and jumping out of it just before it drove directly into a tornado. The truck carried the fictional observing system Dorothy, which consisted of hundreds of lightweight probes that were sucked up by the tornado. The Penn State approach to obtaining aboveground in situ observations in storms is less hair-raising!

[4] Some of the balloons were inflated prior to the mission in order to expedite the launch process once a storm had been targeted. However, there are risks in preinflating balloons, given that it rarely is certain that there will be a targetable storm even just a few hours prior to a deployment. Because latex balloons are porous to helium, it is not possible to "carry over" preinflated balloons to another day in the event that no targetable storms are identified.

the launch frequency could be greatly increased by adding a second team (i.e., a second van), and by adding an extra operator to each team. It would be advantageous to have this third individual continuously monitor the storm's evolution and position, as well as the data collection in progress. In the May 2017 field testing, such monitoring was done by the two operators while they performed the other critical functions described above.

27 May 2017. Extreme instability was present on 27 May 2017. A sounding launched in southern Oklahoma by an NSSL team affiliated with the RiVorS project had a surface-based convective available potential energy (CAPE) of 7900 J kg^{-1} and mixed-layer CAPE of 6400 J kg^{-1} (the latter is computed by lifting an air parcel having the mean potential temperature and water vapor mixing ratio of the lowest 1 km). Relatively strong vertical wind shear was present within the lower half of the troposphere; the 0–6-km shear present on the aforementioned NSSL sounding was 27 m s^{-1}. However, the vertical shear within the boundary layer was somewhat modest by

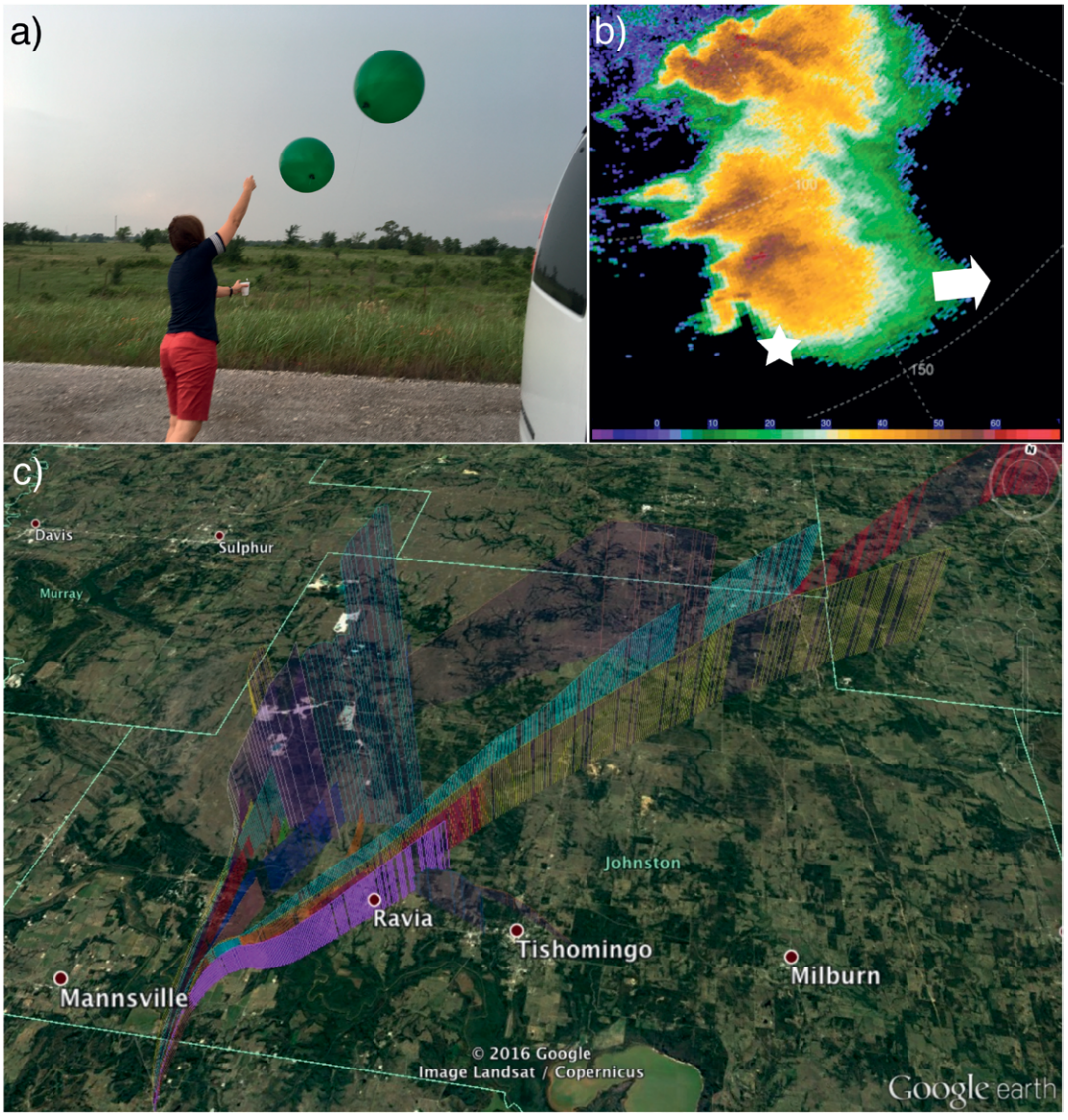

Fig. 2. (a) Photo of one of the authors (Y. Richardson) launching a two-balloon probe into a supercell thunderstorm near Mannsville at 2357 UTC 27 May 2017. (Photo taken by P. Markowski.) (b) WSR-88D reflectivity image [0.5° scan, Oklahoma City, OK (KTLX) radar] at 0049 UTC 28 May. The deployment location is indicated with a white star, and the direction of the storm's motion is indicated with a white arrow. (c) Ground-relative trajectories of the probes that were launched from 2357 UTC 27 May to 0115 UTC 28 May (different colors are used only to make the trajectories easier to visualize). Occasional gaps in the vertical lines along the trajectories indicate where intermittent data dropouts occurred. (Imagery courtesy of Google Earth.)

severe storm standards (<10 m s^{-1}), which might be why a major tornado outbreak failed to develop.

During the 2345 UTC 27 May–0115 UTC 28 May period, 18 probes were launched from near Mannsville along the track of the southern edge of a supercell thunderstorm's forward-flank precipitation region (Fig. 2). Each probe was tracked for 10–45 min, with the duration depending on a probe's whereabouts and whether it was collecting scientifically valuable data. Several of the probes sampled the forward-flank temperature gradients long known to be crucial to tornado formation in supercell storms (Fig. 3). These

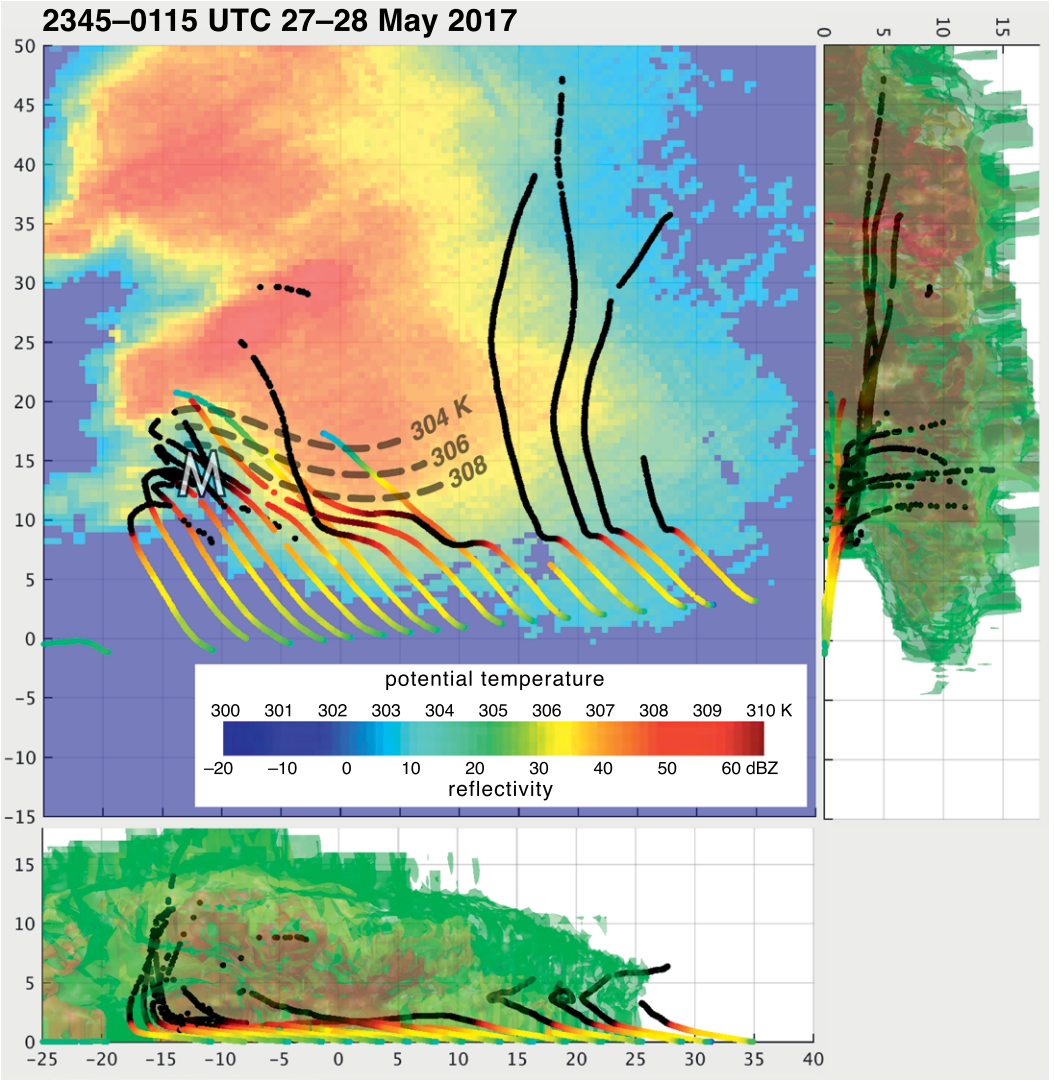

Fig. 3. Storm-relative probe trajectories from 2345 UTC 27 May to 0115 UTC 28 May 2017 through a supercell thunderstorm near Mannsville. Probe trajectories were converted to a storm-relative reference frame by subtracting a storm motion of (11.0, 1.0) m s^{-1}. (top left) Trajectories are shown along the *x*–*y* plane and are overlaid on a WSR-88D reflectivity image from the KTLX radar at 0035 UTC. Trajectories are colored according to the potential temperature sampled. Both the potential temperature and reflectivity scales are indicated in the legend. Potential temperatures greater than 310 K are colored black; the potential temperature scale only goes to 310 K (potential temperatures exceeding 360 K were measured at upper levels within the updraft) in order to emphasize low-altitude horizontal variations in potential temperature, as opposed to vertical variations in potential temperature. The gray dashed lines are manually analyzed isentropes at an altitude of 1 km AGL, which depict the horizontal gradient at that level. The "M" indicates the approximate position of the storm's mesocyclone. (bottom),(top right) Vertical cross sections in the *x*–*z* and *y*–*z* planes, respectively, are also shown. The green, yellow, and red isosurfaces are reflectivities of 25, 35, and 45 dBZ, respectively. All axis labels indicate distances (km).

are the first-ever observations characterizing these gradients aloft. At an altitude of 1 km AGL, the probes sampled a horizontal potential temperature gradient of 1°C km^{-1} within an approximately 5-km-wide by 15-km-long corridor along the southern fringe of the forward-flank precipitation region (note the dashed contours overlaid in Fig. 3); the horizontal gradient of density potential temperature, a more accurate measure of buoyancy that includes the effects of hydrometeors, would likely be larger given how the radar reflectivity increases in the direction in which potential temperature decreases.

One aspect of the deployment that could have been better was the fact that the separation altitude for the first four probes was too high (i.e., two balloons remained attached to the sondes for too long). The altitude was set to 2 km in anticipation that the probes would quickly encounter the storm's forward-flank precipitation, and that it would be desirable to have them attain an altitude of 2 km prior to their expected descent through the forward-flank precipitation–downdraft region. Instead, these first four probes experienced only very light precipitation by that time and continued rising to altitudes of 4–6 km as they traversed the storm's forward flank even after one balloon was released from each probe. We suspect that if a lower separation altitude had been used for the first few probes, they likely would have been pulled more toward the updraft and better sampled the thermodynamic fields along the long axis of the forward-flank precipitation region, as did probes launched later in time using a lower separation altitude (the separation altitude was lowered to 1 km once it was noticed that the first few probes had gained more altitude than desired).

Though it was not our goal, some probes serendipitously sampled the storm's updraft and reached altitudes in excess of 13 km AGL (Fig. 3). One probe recorded a 24-s-average ascent rate[5] of 53 m s^{-1} between 9 and 10 km AGL. It is possible that the vertical velocity of the air would have been a few meters per second greater, given that our small balloons often burst by the time they attain such altitudes (i.e., it is possible that the probe was falling relative to the air at the time the large ascent rates were observed).

31 May 2017. Somewhat weak instability (mixed-layer CAPE generally less than 1000 J kg^{-1}) and modest wind shear over the lower half of the troposphere (generally less than 25 m s^{-1}) were present on 31 May in the western half of Kansas. However, immediately north of a northward-moving outflow boundary, large low-level wind shear (0–3-km storm-relative helicity of roughly 400 J kg^{-1}) was observed on a sounding launched by an NSSL mobile sounding facility. A supercell thunderstorm developed within this relatively narrow corridor of favorable conditions.

From 2351 UTC 31 May to 0115 UTC 1 June, 24 probes were launched from near Ransom, Kansas, located on the southeast flank of the storm (Fig. 4). Even better sampling of the storm's low-level outflow was achieved than on 27 May (Fig. 5). The critical areas immediately northeast of the low-altitude mesocyclone were well sampled by a dozen of the probes, most of which sampled this region in the 500–2000 m AGL layer. The air within the precipitation region in this layer was generally 4°–7°C cooler than the air at similar altitudes sampled in the inflow on the southeast flank of the storm (the density potential temperature deficits would have been a few degrees larger, given the presence of heavy precipitation where the lowest temperatures were observed). A few probes also sampled the outflow and associated downdraft region to the immediate rear of the mesocyclone.

LOOKING AHEAD. Going forward, we hope to combine the aboveground thermodynamic observations with the ground-based mobile mesonet observations obtained by RiVorS into a more comprehensive analysis of the three-dimensional buoyancy field. Mobile radar data from the NSSL X-band, dual-polarization radar (NOXP; Melnikov et al. 2009; Palmer et al. 2009) also are available on 27 and 31 May, as are mobile radar data on 27 May from the Doppler on Wheels radars of the Center for Severe Weather Research (Wurman et al. 1997; Wurman 2001). We also plan to conduct observing system simulation experiments (OSSEs) in order to refine our observing strategy and quantify the impact of the thermodynamic observations.

We are optimistic that the improved three-dimensional sampling of thermodynamic fields in storms afforded by the airborne probes might benefit storm analyses obtained via the popular ensemble Kalman filter (EnKF) approach, which has been used for diagnostic studies of storms from past field experiments (Dowell et al. 2004; Potvin et al. 2013; Tanamachi et al. 2013; Marquis et al. 2014, 2016; Calhoun et al. 2014; Skinner et al. 2015). These analyses typically provide valuable depictions of the evolution of the three-dimensional wind field.

[5] A 24-s average was used owing to a brief data dropout while the probe experienced its most violent upward acceleration.

However, their depictions of the evolution of the accompanying thermodynamic fields is often questionable, in large part owing to the thermodynamic observations being both sparse and limited to the surface, and also because of the large sensitivity of the model forecasts to the model's microphysics parameterization.

In the not-so-distant future, it is likely that advances in technology will allow us to track not a few dozen probes simultaneously with a pair of receivers, but several hundred probes. Moreover, the mass of the probes will likely be reduced by more than 50%, allowing smaller balloons to be used, which would lessen the amount of time required to prepare each

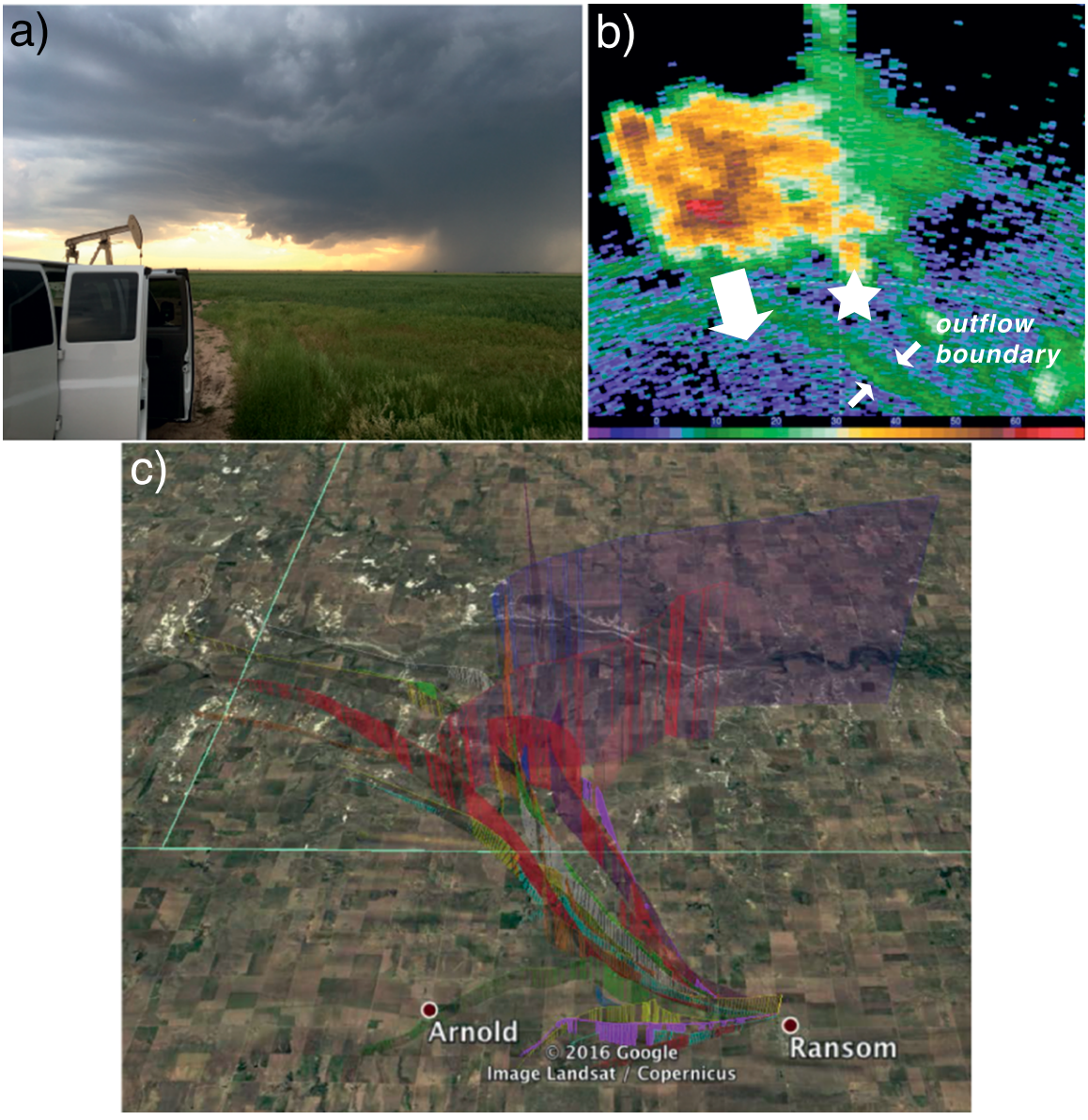

Fig. 4. (a) Photo of the supercell storm near Ransom at 0032 UTC 1 Jun, looking northwest. (Photo taken by Y. Richardson.) The van from which the probes were launched is visible in the foreground. (b) WSR-88D reflectivity image [0.5° scan, Dodge City, KS (KDDC), radar] at 0030 UTC 1 Jun. The deployment location is indicated with a white star, and the direction of the storm's motion is indicated with a thick white arrow. The location of the outflow boundary referenced in the text also is indicated. (c) Ground-relative trajectories of the probes that were launched from 2351 UTC 31 May to 0115 UTC 1 Jun (different colors are used only to make the trajectories easier to visualize). Occasional gaps in the vertical lines along the trajectories indicate where intermittent data dropouts occurred. (Imagery courtesy of Google Earth.)

sonde for launch, thereby increasing the launch frequency and total number of probes flown through a storm. We also are exploring additional strategies for reducing sonde preparation times.

It is hard not to be excited by what the future holds. One can safely assume that aboveground thermodynamic observations from in situ platforms will become increasingly common in the next decade, owing to advances in UAV technology (including autonomous flight), the proliferation of inexpensive drones (e.g., quadcopters), communications, and materials science (advances in materials science will improve the biodegradability of probes), and perhaps even additional relaxation of FAA regulations. In the meantime, the "two balloon" sondes used as pseudo-Lagrangian drifters are a viable way to obtain thermodynamic observations above the ground in convective storms. The versatility of the observing system extends beyond severe storms applications into any area of mesoscale meteorology in which a large array of aboveground, in situ thermodynamic observations is needed.

ACKNOWLEDGMENTS. The success of our first missions would not have been possible without the assistance of many individuals: Dave Stensrud (PSU), Abigail Smith

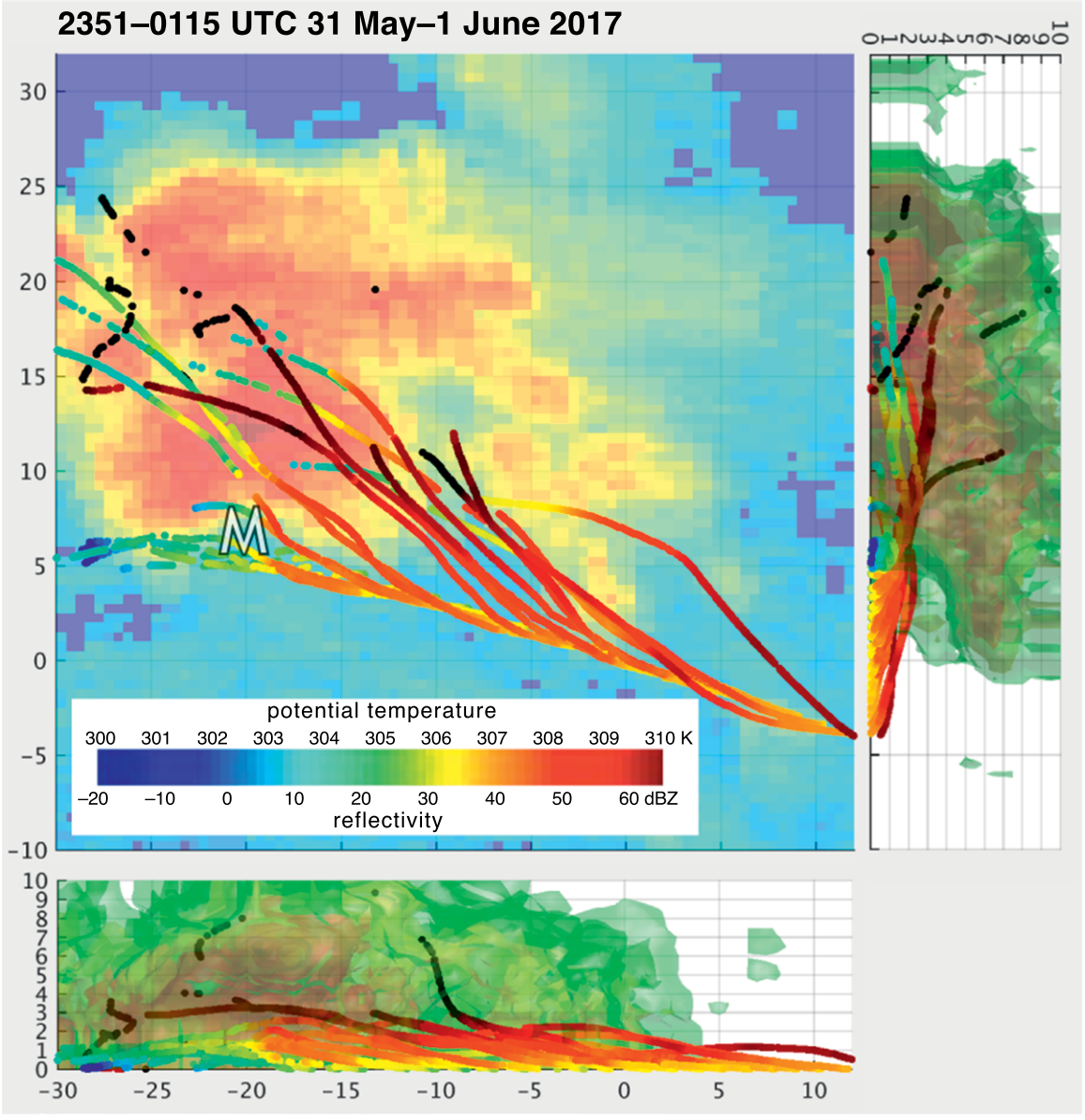

Fig. 5. As in Fig. 3, but for a supercell storm near Ransom during the 2351 UTC 31 May–0115 UTC 1 Jun period. Probe trajectories were converted to a storm-relative reference frame by subtracting a storm motion of (7.0, −2.3) m s^{-1}.

(PSU), Shawn Murdzek (PSU), Marisa Ferger (PSU), Sherman Fredrickson (NSSL), Sean Waugh (NSSL), and Erik Rasmussen (NSSL). We are grateful for the financial support of the National Science Foundation's Physical and Dynamic Meteorology Program (Award AGS-1536460) and Program Director Chungu Lu. Seed funding also was provided by Penn State's Institutes of Energy and the Environment (Interim Director Jenni Evans and Director Tom Richard), and Penn State's College of Earth and Mineral Sciences (Dean Bill Easterling), via the college's Paul Robertson Fund. We also thank Chris Weiss (Texas Tech University) and an anonymous reviewer for their critical reviews of this article.

REFERENCES

Beck, J. R., J. L. Schroeder, and J. M. Wurman, 2006: High-resolution, dual-Doppler analyses of the 29 May 2001 Kress, Texas, cyclic supercell. *Mon. Wea. Rev.*, **134**, 3125–3148, https://doi.org/10.1175/MWR3246.1.

Betten, D. P., M. I. Biggerstaff, and L. J. Wicker, 2017: A trajectory mapping technique for the visualization and analysis of three-dimensional flow in supercell storms. *J. Atmos. Oceanic Technol.*, **34**, 33–49, https://doi.org/10.1175/JTECH-D-16-0043.1.

Brandes, E. A., 1984: Relationships between radar-derived thermodynamic variables and tornadogenesis. *Mon. Wea. Rev.*, **112**, 1033–1052, https://doi.org/10.1175/1520-0493(1984)112<1033:RBRDTV>2.0.CO;2.

Bryan, G. H., and M. D. Parker, 2010: Observations of a squall line and its near environment using high-frequency rawinsonde launches during VORTEX2. *Mon. Wea. Rev.*, **138**, 4076–4097, https://doi.org/10.1175/2010MWR3359.1.

——, and H. Morrison, 2012: Sensitivity of a simulated squall line to horizontal resolution and parameterization of microphysics. *Mon. Wea. Rev.*, **140**, 202–225, https://doi.org/10.1175/MWR-D-11-00046.1.

Calhoun, K. M., D. R. MacGorman, C. L. Ziegler, and M. I. Biggerstaff, 2013: Evolution of lightning activity and storm charge relative to dual-Doppler analysis of a high-precipitation supercell storm. *Mon. Wea. Rev.*, **141**, 2199–2223, https://doi.org/10.1175/MWR-D-12-00258.1.

——, E. R. Mansell, D. R. MacGorman, and D. C. Dowell, 2014: Numerical simulations of lightning and storm charge of the 29–30 May 2004 Geary, Oklahoma, supercell thunderstorm using EnKF mobile radar data assimilation. *Mon. Wea. Rev.*, **142**, 3977–3997, https://doi.org/10.1175/MWR-D-13-00403.1.

Coniglio, M. C., and D. J. Stensrud, 2001: Simulation of a progressive derecho using composite initial conditions. *Mon. Wea. Rev.*, **129**, 1593–1616, https://doi.org/10.1175/1520-0493(2001)129<1593:SOAPDU>2.0.CO;2.

Correia, J., Jr., and R. W. Arritt, 2008: Thermodynamic properties of mesoscale convective systems observed during BAMEX. *Mon. Wea. Rev.*, **136**, 4242–4271, https://doi.org/10.1175/2008MWR2284.1.

Davenport, C. E., and M. D. Parker, 2015: Observations of the 9 June 2009 dissipating supercell from VORTEX2. *Wea. Forecasting*, **30**, 368–388, https://doi.org/10.1175/WAF-D-14-00087.1.

Davies-Jones, R., 2015: A review of supercell and tornado dynamics. *Atmos. Res.*, **158–159**, 274–291, https://doi.org/10.1016/j.atmosres.2014.04.007.

Dawson, D. T., M. Xue, J. A. Milbrandt, and M. K. Yau, 2010: Comparison of evaporation and cold pool development between single-moment and multimoment bulk microphysics schemes in idealized simulations of tornadic thunderstorms. *Mon. Wea. Rev.*, **138**, 1152–1171, https://doi.org/10.1175/2009MWR2956.1.

——, ——, ——, and A. Shapiro, 2015: Sensitivity of real-data simulations of the 3 May 1999 Oklahoma City tornadic supercell and associated tornadoes to multimoment microphysics. Part I: Storm- and tornado-scale numerical forecasts. *Mon. Wea. Rev.*, **143**, 2241–2265, https://doi.org/10.1175/MWR-D-14-00279.1.

Dowell, D. C., and H. B. Bluestein, 2002: The 8 June 1995 McLean, Texas, storm. Part I: Observations of cyclic tornadogenesis. *Mon. Wea. Rev.*, **130**, 2626–2648, https://doi.org/10.1175/1520-0493(2002)130<2626:TJMTSP>2.0.CO;2.

——, F. Zhang, L. J. Wicker, C. Snyder, and N. A. Crook, 2004: Wind and temperature retrievals in the 17 May 1981 Arcadia, Oklahoma, supercell: Ensemble Kalman filter experiments. *Mon. Wea. Rev.*, **132**, 1982–2005, https://doi.org/10.1175/1520-0493(2004)132<1982:WATRIT>2.0.CO;2.

Engerer, N. A., D. J. Stensrud, and M. C. Coniglio, 2008: Surface characteristics of observed cold pools. *Mon. Wea. Rev.*, **136**, 4839–4849, https://doi.org/10.1175/2008MWR2528.1.

Frame, J., P. Markowski, Y. Richardson, J. Straka, and J. Wurman, 2009: Polarimetric and dual-Doppler radar observations of the Lipscomb County, Texas, supercell thunderstorm on 23 May 2002. *Mon. Wea. Rev.*, **137**, 544–561, https://doi.org/10.1175/2008MWR2425.1.

Gal-Chen, T., 1978: A method for the initialization of the anelastic equations: Implications for matching models with observations. *Mon. Wea. Rev.*, **106**, 587–606, https://doi.org/10.1175/1520-0493(1978)106<0587:AMFTIO>2.0.CO;2.

Gilmore, M. S., J. M. Straka, and E. N. Rasmussen, 2004: Precipitation and evolution sensitivity in simulated deep convective storms: Comparisons between liquid-only and simple ice and liquid phase microphysics. *Mon. Wea. Rev.*, **132**, 1897–1916, https://doi.org/10.1175/1520-0493(2004)132<1897:PAESIS>2.0.CO;2.

Grzych, M. L., B. D. Lee, and C. A. Finley, 2007: Thermodynamic analysis of supercell rear-flank downdrafts from Project ANSWERS. *Mon. Wea. Rev.*, **135**, 240–246, https://doi.org/10.1175/MWR3288.1.

Hane, C. E., R. B. Wilhelmson, and T. Gal-Chen, 1981: Retrieval of thermodynamic variables within deep convective clouds: Experiments in three dimensions. *Mon. Wea. Rev.*, **109**, 564–576, https://doi.org/10.1175/1520-0493(1981)109<0564:ROTVWD>2.0.CO;2.

Hauser, D., F. Roux, and P. Amayenc, 1988: Comparison of two methods for the retrieval of thermodynamic and microphysical variables from Doppler radar measurements: Application to the case of a tropical squall line. *J. Atmos. Sci.*, **45**, 1285–1303, https://doi.org/10.1175/1520-0469(1988)045<1285:COTMFT>2.0.CO;2.

Hirth, B. D., J. L. Schroeder, and C. C. Weiss, 2008: Surface analysis of the rear-flank downdraft outflow in two tornadic supercells. *Mon. Wea. Rev.*, **136**, 2344–2363, https://doi.org/10.1175/2007MWR2285.1.

Houston, A. L., B. Argrow, J. Elston, J. Lahowetz, E. W. Frew, and P. C. Kennedy, 2012: The Collaborative Colorado–Nebraska Unmanned Aircraft System Experiment. *Bull. Amer. Meteor. Soc.*, **93**, 39–54, https://doi.org/10.1175/2011BAMS3073.1.

James, R. P., P. M. Markowski, and J. M. Fritsch, 2006: Bow echo sensitivity to ambient moisture and cold pool strength. *Mon. Wea. Rev.*, **134**, 950–964, https://doi.org/10.1175/MWR3109.1.

Klees, A. M., Y. P. Richardson, P. M. Markowski, C. Weiss, J. M. Wurman, and K. K. Kosiba, 2016: Comparison of the tornadic and nontornadic supercells intercepted by VORTEX2 on 10 June 2010. *Mon. Wea. Rev.*, **144**, 3201–3231, https://doi.org/10.1175/MWR-D-15-0345.1.

Kosiba, K., J. Wurman, Y. Richardson, P. Markowski, P. Robinson, and J. Marquis, 2013: Genesis of the Goshen County, Wyoming, tornado (5 June 2009). *Mon. Wea. Rev.*, **141**, 1157–1181, https://doi.org/10.1175/MWR-D-12-00056.1.

Majcen, M., P. Markowski, Y. Richardson, D. Dowell, and J. Wurman, 2008: Multipass objective analyses of radar data. *J. Atmos. Oceanic Technol.*, **25**, 1845–1858, https://doi.org/10.1175/2008JTECHA1089.1.

Markowski, P. M., and Y. P. Richardson, 2009: Tornadogenesis: Our current understanding, forecasting considerations, and questions to guide future research. *Atmos. Res.*, **93**, 3–10, https://doi.org/10.1016/j.atmosres.2008.09.015.

——, and ——, 2014: The influence of environmental low-level shear and cold pools on tornadogenesis: Insights from idealized simulations. *J. Atmos. Sci.*, **71**, 243–275, https://doi.org/10.1175/JAS-D-13-0159.1.

——, J. M. Straka, and E. N. Rasmussen, 2002: Direct surface thermodynamic observations within the rear-flank downdrafts of nontornadic and tornadic supercells. *Mon. Wea. Rev.*, **130**, 1692–1721, https://doi.org/10.1175/1520-0493(2002)130<1692:DSTOWT>2.0.CO;2.

——, M. Majcen, Y. P. Richardson, J. Marquis, and J. Wurman, 2011: Characteristics of the wind field in three nontornadic low-level mesocyclones observed by the Doppler On Wheels radars. *Electron. J. Severe Storms Meteor.*, **6** (3), www.ejssm.org/ojs/index.php/ejssm/article/viewArticle/75.

——, and Coauthors, 2012: The pretornadic phase of the Goshen County, Wyoming, supercell of 5 June 2009 intercepted by VORTEX2. Part I: Evolution of kinematic and surface thermodynamic fields. *Mon. Wea. Rev.*, **140**, 2887–2915, https://doi.org/10.1175/MWR-D-11-00336.1.

Marquis, J. N., Y. P. Richardson, J. M. Wurman, and P. M. Markowski, 2008: Single- and dual-Doppler analysis of a tornadic vortex and surrounding storm-scale flow in the Crowell, Texas, supercell of 30 April 2000. *Mon. Wea. Rev.*, **136**, 5017–5043, https://doi.org/10.1175/2008MWR2442.1.

——, ——, P. Markowski, D. Dowell, and J. Wurman, 2012: Tornado maintenance investigated with high-resolution dual-Doppler and EnKF analysis. *Mon. Wea. Rev.*, **140**, 3–27, https://doi.org/10.1175/MWR-D-11-00025.1.

——, ——, ——, ——, ——, K. Kosiba, and P. Robinson, 2014: An investigation of the Goshen County, Wyoming, tornadic supercell of 5 June 2009 using EnKF assimilation of mobile radar data collected during VORTEX2. Part I: Experiment design and verification of the EnKF analyses. *Mon. Wea. Rev.*, **142**, 530–554, https://doi.org/10.1175/MWR-D-13-00007.1.

——, ——, ——, ——, ——, and ——, 2016: An investigation of the Goshen County, Wyoming, tornadic supercell of 5 June 2009 using EnKF assimilation of mobile mesonet and radar observations collected during VORTEX2. Part II: Mesocyclone-scale processes affecting tornado formation, maintenance, and decay. *Mon. Wea. Rev.*, **144**, 3441–3463, https://doi.org/10.1175/MWR-D-15-0411.1.

Melnikov, V., D. Zrnić, A. Ryzhkov, A. Zaharai, and J. Carter, 2009: Validation of attenuation correction

at X band performed with collocated S-band polarimetric radar. *34th Conf. on Radar Meteorology*, Williamsburg, VA, Amer. Meteor. Soc., 11A.5, https://ams.confex.com/ams/34Radar/techprogram/paper_155322.htm.

Palmer, R. D., and Coauthors, 2009: Weather radar education at the University of Oklahoma: An integrated interdisciplinary approach. *Bull. Amer. Meteor. Soc.*, **90**, 1277–1282, https://doi.org/10.1175/2009BAMS2738.1.

Potvin, C. K., L. J. Wicker, M. I. Biggerstaff, D. Betten, and A. Shapiro, 2013: Comparison between dual-Doppler and EnKF storm-scale wind analyses: The 29–30 May 2004 Geary, Oklahoma, supercell thunderstorm. *Mon. Wea. Rev.*, **141**, 1612–1628, https://doi.org/10.1175/MWR-D-12-00308.1.

Riganti, C. J., and A. L. Houston, 2017: Rear-flank outflow dynamics and thermodynamics in the 10 June 2010 Last Chance, Colorado, supercell. *Mon. Wea. Rev.*, **145**, 2487–2504, https://doi.org/10.1175/MWR-D-16-0128.1.

Roberts, B., M. Xue, A. D. Schenkman, and D. T. Dawson II, 2016: The role of surface drag in tornadogenesis within an idealized supercell simulation. *J. Atmos. Sci.*, **73**, 3371–3395, https://doi.org/10.1175/JAS-D-15-0332.1.

Rotunno, R., J. B. Klemp, and M. L. Weisman, 1988: A theory for strong, long-lived squall lines. *J. Atmos. Sci.*, **45**, 463–485, https://doi.org/10.1175/1520-0469(1988)045<0463:ATFSLL>2.0.CO;2.

Schenkman, A. D., M. Xue, and A. Shapiro, 2012: Tornadogenesis in a simulated mesovortex within a mesoscale convective system. *J. Atmos. Sci.*, **69**, 3372–3390, https://doi.org/10.1175/JAS-D-12-038.1.

——, ——, and M. Hu, 2014: Tornadogenesis in a high-resolution simulation of the 8 May 2003 Oklahoma City supercell. *J. Atmos. Sci.*, **71**, 130–154, https://doi.org/10.1175/JAS-D-13-073.1.

Shabbott, C. J., and P. M. Markowski, 2006: Surface in situ observations within the outflow of forward-flank downdrafts of supercell thunderstorms. *Mon. Wea. Rev.*, **134**, 1422–1441, https://doi.org/10.1175/MWR3131.1.

Skinner, P. S., C. C. Weiss, M. M. French, H. B. Bluestein, P. M. Markowski, and Y. P. Richardson, 2014: VORTEX2 observations of a low-level mesocyclone with multiple internal rear-flank downdraft momentum surges in the 18 May 2010 Dumas, Texas, supercell. *Mon. Wea. Rev.*, **142**, 2935–2960, https://doi.org/10.1175/MWR-D-13-00240.1.

——, ——, L. J. Wicker, C. K. Potvin, and D. C. Dowell, 2015: Forcing mechanisms for an internal rear-flank downdraft momentum surge in the 18 May 2010 Dumas, Texas, supercell. *Mon. Wea. Rev.*, **143**, 4305–4330, https://doi.org/10.1175/MWR-D-15-0164.1.

Snook, N., and M. Xue, 2008: Effects of microphysical drop size distribution on tornadogenesis in supercell thunderstorms. *Geophys. Res. Lett.*, **35**, L24803, https://doi.org/10.1029/2008GL035866.

Stensrud, D. J., M. C. Coniglio, R. P. Davies-Jones, and J. S. Evans, 2005: Comments on "'A theory for strong long-lived squall lines' revisited." *J. Atmos. Sci.*, **62**, 2989–2996, https://doi.org/10.1175/JAS3514.1.

Straka, J. M., E. N. Rasmussen, and S. E. Fredrickson, 1996: A mobile mesonet for finescale meteorological observations. *J. Atmos. Oceanic Technol.*, **13**, 921–936, https://doi.org/10.1175/1520-0426(1996)013<0921:AMMFFM>2.0.CO;2.

Tanamachi, R. L., L. J. Wicker, D. C. Dowell, H. B. Bluestein, D. T. Dawson II, and M. Xue, 2013: EnKF assimilation of high-resolution, mobile Doppler radar data of the 4 May 2007 Greensburg, Kansas, supercell into a numerical cloud model. *Mon. Wea. Rev.*, **141**, 625–648, https://doi.org/10.1175/MWR-D-12-00099.1.

Trapp, R. J., 1999: Observations of nontornadic low-level mesocyclones and attendant tornadogenesis failure during VORTEX. *Mon. Wea. Rev.*, **127**, 1693–1705, https://doi.org/10.1175/1520-0493(1999)127<1693:OONLLM>2.0.CO;2.

Wakimoto, R. M., and N. T. Atkins, 1996: Observations on the origins of rotation: The Newcastle tornado during VORTEX94. *Mon. Wea. Rev.*, **124**, 384–407, https://doi.org/10.1175/1520-0493(1996)124<0384:OOTOOR>2.0.CO;2.

——, and H. Cai, 2000: Analysis of a nontornadic storm during VORTEX95. *Mon. Wea. Rev.*, **128**, 565–592, https://doi.org/10.1175/1520-0493(2000)128<0565:AOANSD>2.0.CO;2.

——, C. Liu, and H. Cai, 1998: The Garden City, Kansas, storm during VORTEX95. Part I: Overview of the storm life cycle and mesocyclogenesis. *Mon. Wea. Rev.*, **126**, 372–392, https://doi.org/10.1175/1520-0493(1998)126<0372:TGCKSD>2.0.CO;2.

Waugh, S., and S. E. Fredrickson, 2010: An improved aspirated temperature system for mobile meteorological observations, especially in severe weather. *25th Conf. on Severe Local Storms*, Denver, CO, Amer. Meteor. Soc., P5.2.

Weisman, M. L., and R. Rotunno, 2004: "A theory for strong long-lived squall lines" revisited. *J. Atmos. Sci.*, **61**, 361–382, https://doi.org/10.1175/1520-0469(2004)061<0361:ATFSLS>2.0.CO;2.

——, and ——, 2005: Reply. *J. Atmos. Sci.*, **62**, 2997–3002, https://doi.org/10.1175/JAS3515.1.

Weiss, C. C., and J. L. Schroeder, 2008: StickNet: A new portable, rapidly deployable surface observation system. *Bull. Amer. Meteor. Soc.*, **89**, 1502–1503.

——, D. C. Dowell, J. L. Schroeder, P. S. Skinner, A. E. Reinhart, P. M. Markowski, and Y. P. Richardson, 2015: A comparison of near-surface buoyancy and baroclinity across three VORTEX2 supercell intercepts. *Mon. Wea. Rev.*, **143**, 2736–2753, https://doi.org/10.1175/MWR-D-14-00307.1.

Wurman, J., 2001: The DOW mobile multiple Doppler network. *30th Int. Conf. on Radar Meteorology*, Munich, Germany, Amer. Meteor. Soc., P3.3, http://ams.confex.com/ams/pdfpapers/21572.pdf.

——, J. Straka, E. Rasmussen, M. Randall, and A. Zahrai, 1997: Design and deployment of a portable, pencil-beam, pulsed, 3-cm Doppler radar. *J. Atmos. Oceanic Technol.*, **14**, 1502–1512, https://doi.org/10.1175/1520-0426(1997)014<1502:DADOAP>2.0.CO;2.

——, Y. Richardson, C. Alexander, S. Weygandt, and P. F. Zhang, 2007a: Dual-Doppler analysis of winds and vorticity budget terms near a tornado. *Mon. Wea. Rev.*, **135**, 2392–2405, https://doi.org/10.1175/MWR3404.1.

——, ——, ——, ——, and ——, 2007b: Dual-Doppler and single-Doppler analysis of a tornadic storm undergoing mergers and repeated tornadogenesis. *Mon. Wea. Rev.*, **135**, 736–758, https://doi.org/10.1175/MWR3276.1.

——, K. A. Kosiba, P. Markowski, Y. Richardson, D. Dowell, and P. Robinson, 2010: Finescale and dual-Doppler analysis of tornado intensification, maintenance, and dissipation in the Orleans, Nebraska, tornadic supercell. *Mon. Wea. Rev.*, **138**, 4439–4455, https://doi.org/10.1175/2010MWR3330.1.

Xu, X., M. Xue, and Y. Wang, 2015: The genesis of mesovortices within a real-data simulation of a bow echo system. *J. Atmos. Sci.*, **72**, 1963–1986, https://doi.org/10.1175/JAS-D-14-0209.1.

Ziegler, C. L., E. N. Rasmussen, T. R. Shepherd, A. I. Watson, and J. M. Straka, 2001: The evolution of low-level rotation in the 29 May 1994 Newcastle–Graham, Texas, storm complex during VORTEX. *Mon. Wea. Rev.*, **129**, 1339–1368, https://doi.org/10.1175/1520-0493(2001)129<1339:TEOLLR>2.0.CO;2.